

# Interfacing Superconducting Qubits with Cryogenic Logic: Readout

Caleb Howington  
B.L.T. Plourde  
Department of Physics  
Syracuse University  
Syracuse, New York 13244  
Email: bplourde@syr.edu

A. Opremcak  
R. McDermott  
Department of Physics  
University of Wisconsin-Madison  
Madison, Wisconsin 53706

A. Kirichenko  
O.A. Mukhanov  
HYPRES, Inc.  
Elmsford, New York 10523

**Abstract**—As superconducting quantum processors increase in size and complexity, the scalability of standard techniques for qubit control and readout becomes a limiting factor. Replacing room temperature analog components with cryogenic digital components could allow for the realization of systems **well beyond the current state-of-the-art qubit arrays with tens of qubits**. The standard technique for performing a qubit measurement with heterodyne readout uses a quantum-limited cryogenic amplifier chain and requires bulky microwave components inside the refrigerator with multiple control lines and pump signals. Additionally, the result is only accessible in software at room temperature. An alternative method for measuring qubits involves mapping the qubit state onto the photon occupation in a microwave cavity, followed by subsequent photon detection using a Josephson Photomultiplier (JPM). The JPM measures the qubit and stores the result in a classical circulating current. To make use of this result, we can leverage existing single flux quantum (SFQ) circuitry. An underdamped Josephson Transmission Line (JTL) can be coupled to the JPM and fluxons traveling along the JTL are accelerated or delayed, depending on the circulating current state of the JPM. This fluxon delay can then be converted to an SFQ logic signal resulting in a digital qubit readout with a proximal microfabricated device, paving the way for cryogenic digital feedback necessary for error-correcting codes.

## I. INTRODUCTION

Superconducting qubits have become a promising basis for a large-scale quantum processor [1], [2]. One vision for a scalable quantum computing architecture leverages cryogenic, classical superconducting control and readout circuitry based on the SFQ (Single Flux Quantum) logic family [3]. SFQ logic has been developed as a high speed, ultra-low power consumption digital technology [4]. One key element of the architecture described in [3], the control of a transmon qubit with SFQ logic [5], has recently been demonstrated [6]. The development of the Josephson Photomultiplier (JPM) [7] has allowed for high-fidelity qubit measurement without the need of heterodyne detection of the microwave cavity coupled to the qubit [8]. One of the key benefits of JPM-based measurement is the accessibility of the qubit measurement result at the same temperature stage of the cryostat as the qubit.

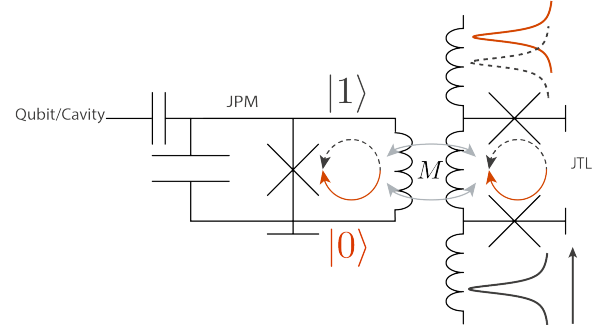


Fig. 1. The JPM measurement process maps the state of the qubit onto the photon occupation of a cavity, and then the occupation of the cavity onto the circulating current of the JPM. Detecting this current with SFQ logic would allow for digital cryogenic feedback with minimal overhead and latency.

## II. QUBIT MEASUREMENT WITH A JOSEPHSON PHOTOMULTIPLIER

Superconducting transmon qubits are conventionally measured using heterodyne detection of a coupled resonator [9]. This method has resulted in measurement fidelities greater than 99% in 500 ns [10] while remaining **Quantum non-demolition (QND)** [9]. However, heterodyne detection requires a significant amount of physical overhead that makes it difficult to scale up to systems with many qubits. The high fidelities achieved in [10] required a near-quantum-limited amplifier, a strong microwave pump tone, bulky and magnetic microwave isolators and circulators to protect the qubit from back-action of the amplifier, a HEMT amplifier at 4 K, and several microwave components for room-temperature processing.

The **JPM** is related to a flux-biased phase qubit [11] that can be tuned in and out of resonance with the readout cavity that is coupled to the qubit. The measurement process consists of mapping the qubit state on to the cavity photon occupation, and then detecting the presence or absence of cavity photons with the JPM. [12]. The result of the qubit measurement is stored in the classical circulating current in the inductor of the JPM. In [8], the final state of the JPM was detected using microwave reflectometry.

Here, we present a scheme to detect the state of the JPM

with ballistic fluxons. By coupling these fluxons to the JPM shunt inductor, we can induce a forward or reverse bias that advances or delays the fluxon propagation. This delay is then converted to an SFQ logic signal for a digital output of the qubit measurement result.

### III. PRIOR WORK

#### A. Fluxon readout of flux qubits




The use of propagating fluxons as a direct probe of the state of a qubit was first investigated theoretically in [13]. Here, a ballistic JTL is coupled directly to a superconducting flux qubit, whose states correspond to different circulating currents [14]. In order to minimize backaction from the JTL on the qubit and thus maintain QND readout, an exceedingly weak coupling strength between the JTL and qubit was required. This prevents the qubit measurement from being performed in a single shot. A full circuit schematic for this approach was developed in [15] and improved in [16], including additional components to detect the induced delay. Recently, this method for measuring flux qubits has been developed further and studied with numerical simulations in [17]–[20]. In addition to these theoretical studies of JTL-based flux qubit readout, an experimental implementation of flux qubit readout using traveling fluxons in an annular Josephson junction was demonstrated in [21].

In contrast to these schemes for direct qubit readout with propagating fluxons in a JTL, the detection of circulating current states from JPM-based qubit measurement has clear advantages. The circulating current being detected in the JPM is one or two orders of magnitude larger than that in a flux qubit. Furthermore, the JPM acts as a buffer between the SFQ circuitry and qubit since, outside of the brief moment when the JPM is on resonance with the qubit cavity, the JPM is otherwise far detuned. Thus, dissipation or noise in the JTL that is coupled to the JPM will not be directly coupled back to the qubit being measured. Finally, because the circulating current states in the JPM following the nearly QND measurement of the qubit are completely classical, the detection of the JPM state with propagating fluxons does not need to be QND.

### IV. DESIGN

Our circuit for converting the state of the JPM to an SFQ signal is related to the earlier work from [13] and [16], for SFQ-based readout of a flux qubit, where the time delay of a propagating fluxon in a coupled ballistic JTL is compared to a reference ballistic JTL. Upon discrimination of the delay, the SFQ output of the measurement result can then be optionally converted to a dc pulse for room-temperature detection.

Conventional RSFQ logic cells operating at 4 K typically utilize Josephson junctions with critical currents on the order of 100  $\mu\text{A}$ . Because the JPM will need to operate at the same low-temperature stage of a dilution refrigerator along with the qubit, utilizing millikelvin SFQ technology will be critical [22]. In addition, because the JPM junction, with  $I_c = 1 \mu\text{A}$ , must be fabricated with the same critical current density as the

SFQ circuitry, critical currents for the SFQ elements will be in the 1–10  $\mu\text{A}$  range. The combination of low- $I_c$  junctions with inductive biasing results in zero static and minimal dynamic power dissipation, thus allowing the circuit to operate at qubit temperatures with a minimal  load on the cryostat. An  analysis of the footprint, heat, and wiring considerations of  circuit as a component of a larger classical qubit interface has been discussed in Section V of [3].

#### A. Coupled ballistic lines

Figure 2 shows the schematic of our circuit for implementing the detection of the state of a JPM following qubit measurement using SFQ circuitry. The design incorporates two ballistic JTLs – one along the top of the schematic and the other along the bottom – with equal and opposite coupling between the central cell of each JTL and the JPM inductor. This arrangement causes the net flux in one of the central JTL cells to increase, thus slowing down the fluxon propagation, while the net flux decreases in the central cell of the other JTL, which speeds up the fluxon propagation there. Thus, this scheme enhances the relative delay between fluxons propagating in the two JTLs. In addition, this results in the flux induced back into the JPM from one passing fluxon to be canceled out by the flux induced by the second fluxon, thus minimizing the flux coupled to the JPM from the JTLs during the measurement. The ballistic lines consist of 12 JTL cells, with parameters  $L_{JTL} = 41 \text{ pH}$  and  $I_c = 2 \mu\text{A}$ . This results in a normalized Josephson length  $\tilde{\lambda}_J = \sqrt{\hbar/2eI_cL_1} = 2 \text{ cells}$ .

A significant enhancement of the relative fluxon delay can be achieved by adding a separate, negative current bias to the final cell of each of the ballistic JTLs. Biasing only this last cell adds to the delay of the delayed fluxon as it travels through the ballistic JTL, but minimally perturbs the other fluxon. This bias current can be used to enhance the fluxon delay by over an order of magnitude with a small mutual inductance (Fig. 3). A 10 pH mutual is targeted to minimize backaction (Section IV-D) while allowing for a sufficient delay ( $> 15 \text{ ps}$ ) to ensure appropriate margins of the DFF.

#### B. Triggering

A standard DC-SFQ converter and splitter are used to launch the fluxons into the ballistic JTLs at the same initial starting time. Combiners are added to both lines so that a reset pulse can be added for the delay detection circuitry. Adding combiners to both lines ensures that the total time delay of both ballistic paths are identical in the absence of a JPM circulating current. In future designs, additional components can be added to reset the delay detection circuitry automatically, making a secondary trigger is unnecessary.

#### C. Delay Detection

The delay detection circuit is modeled after delay demodulation circuitry used in superconducting analog-to-digital converters [23]. Since there are only two possible states of the JPM, the detection circuit only needs a single bit of resolution to distinguish the pulse arrival times. A single D Flip-Flop

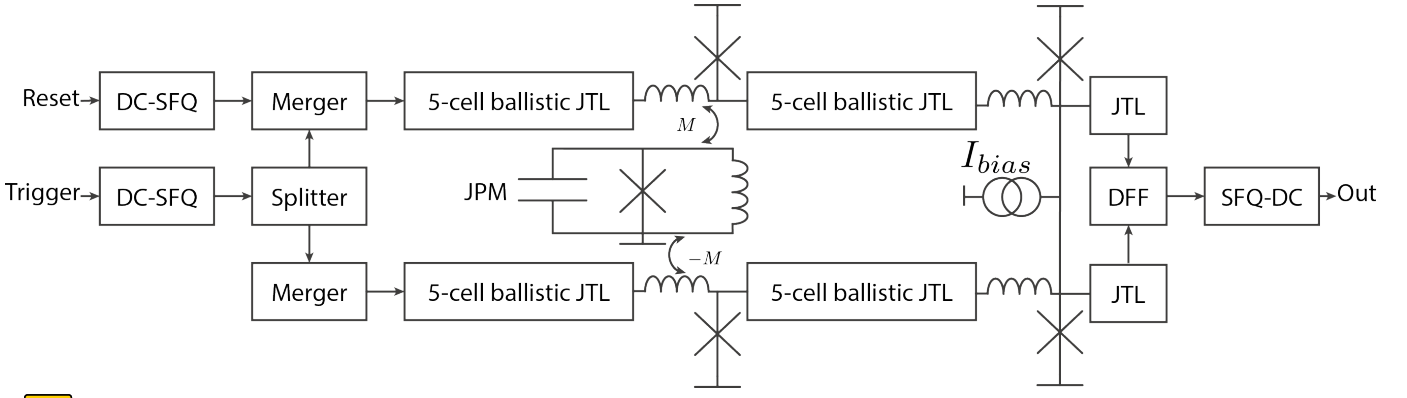


Fig. 1. Circuit diagram of the JPM-SFQ interface and delay-detection circuitry. Other than the JPM control bias, all inputs and outputs are either digital pulses or static current biases.

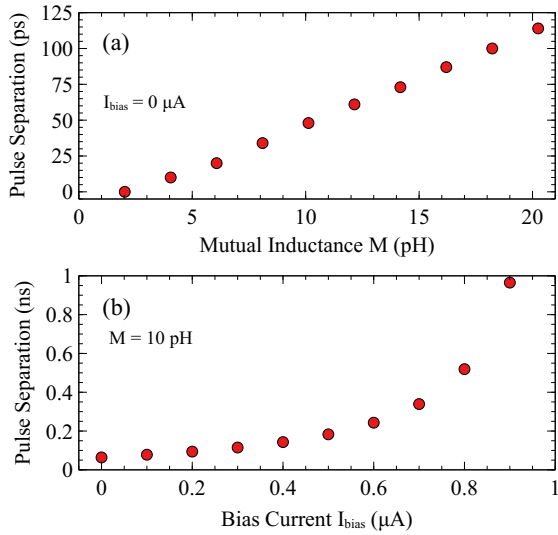


Fig. 2. (a) Dependence of pulse separation on coupling mutual with no bias. (b) Dependence of pulse separation on bias current with a 10 pH mutual inductance. Mutual inductance is targeted at 10 pH.

(DFF) can be used to determine the order of the arriving pulses. If the data pulse arrives first, the following clock pulses produces a logical 1. If the clock pulse arrives first, the following data pulse produces a logical 0 at the output. Sending a reset pulse following this detection resets the DFF, with the resulting output ignored.

#### D. Backaction

Although the backaction requirements are much less severe for detecting the state of a JPM rather than the original schemes for the direct readout of a flux qubit, it is nonetheless important to consider the effects of the ballistic JTLs coupled to the JPM. One concern is that the coupling of the JTLs to the JPM will perturb the tunneling rates of the biased JPM, thus impacting the qubit measurement fidelity of the JPM. Additionally, for sufficiently strong mutual inductances between the JTLs and JPM, fluxons traveling through the

ballistic JTLs could couple enough flux back into the JPM to induce a switching event, thus perturbing the JPM state and coupling noise back into the qubit-cavity through the subsequent ringdown oscillations of the JPM. However, if the coupling mutual is low enough so as not to induce a tunneling event, yet large enough to result in a resolvable fluxon delay, the fluxon-based readout should be considered a non-destructive readout (NDRO) method, with no impact on the state of the JPM or any coupled qubit systems.

We can analyze the coupling of the JPM to the ballistic JTL by modeling the JPM coupled to a single cell of an unbiased, unshunted JTL. The resulting model is essentially two coupled rf SQUIDs with quite different  $\beta_L \equiv 2\pi I_c L / \Phi_0$  parameters: 4.8 for the JPM and 0.01 for the JTL, and effective masses, as determined by the 3 pF shunt capacitor of the JPM and the much smaller, 80 fF self capacitance of the JTL junction. The inductive contribution of the coupled system to the potential energy is given by

$$U_L(\Phi_1, \Phi_2) = -\frac{1}{\beta_M} \left( \frac{\tilde{\Phi}_1^2}{L_1} + \frac{\tilde{\Phi}_2^2}{L_2} - \frac{2M}{L_1 L_2} \tilde{\Phi}_1 \tilde{\Phi}_2 \right) \quad (1)$$

where  $L_1$  is the JPM inductance,  $L_2$  is the JTL inductance,  $\beta_M = (1 - M^2/L_1 L_2)$ , and  $\tilde{\Phi}_i = \Phi_i - \Phi_{i,x}$ . The offset term  $\Phi_{i,x}$  is the externally applied flux and  $\Phi_1$  and  $\Phi_2$  are the total flux in JPM and JTL loops, respectively. The flux added to the coupled JTL cell comes from any residual current bias and can be considered to be 0 for this analysis.

For a realistic set of parameters ( $L_1 = 1$  nH,  $L_2 = 40$  pH,  $M = 10$  pH), the prefactor of the inductive potential term ( $1/\beta_M$ ) is quite nearly unity (0.995), resulting in a negligible change to  $\beta_L$  for the JPM. Additionally, the prefactor of the coupling term in (1) is  $\approx 0.0025$ , and is thus dominated by the diagonal terms in the potential with a negligible contribution to the tunneling behavior of the JPM. The small capacitance of the JTL junction contributes to the kinetic term of the coupled Hamiltonian. However, since the plasma frequency of this junction is on the order of 100 GHz, compared to  $\sim 5$  GHz for the JPM, and with parasitic capacitance between the JPM and JTL negligible, we can neglect any effect of the

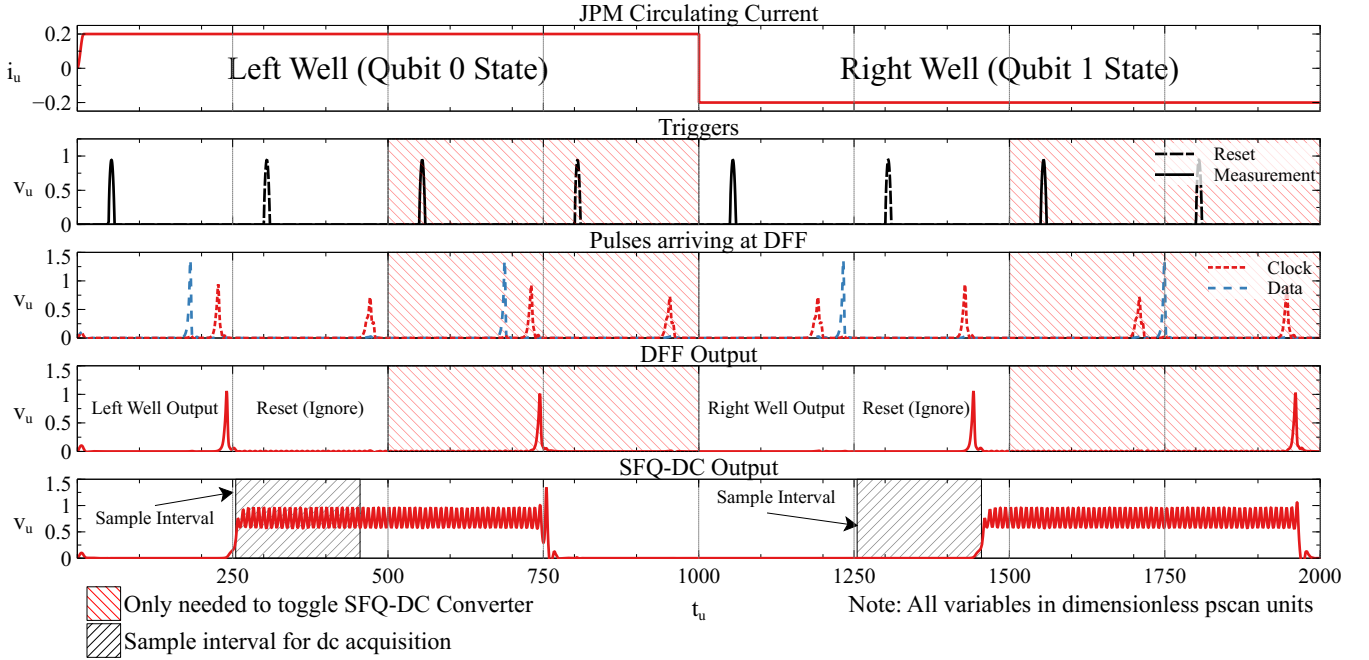


Fig. 4. Simulation results of the JPM-SFQ interface. Panel 1: Circulating current in the JPM, first in the left well (corresponding to one qubit state), and then in the right well (corresponding to the other qubit state). Panel 2: Series of triggers needed to operate the circuit. The solid Measurement pulse triggers the two fluxons that travel down the ballistic JTLs. The dashed Reset pulse resets the DFF. Panel 3: pulses received by the DFF. When the JPM is in the left (right) well, the data (clock) pulse arrives first. Panel 4: Output of the DFF. With the JPM in the left (right) well, the measurement pulse results in a 1 (0), and the reset pulse results in a 0 (1) and is ignored. Panel 5: Output of an optional SFQ-DC converter that can be used to detect the output of the circuit at room temperature. The trigger sequence is repeated in this case (shaded areas) to turn off the SFQ-DC converter after acquisition. **Once the output is acquired, the JPM is reset into its initial well (not shown). The full JPM measurement protocol is outlined in [8].** Note: All units are in dimensionless pscan units.

JTL junction capacitance on the Hamiltonian for the coupled system. If the coupled JTL cell contributes negligibly to the behavior of the JPM, we can also neglect the contributions of the other segments of each ballistic JTL beyond the central unit cell of each one. By keeping the mutual inductance and parasitic capacitance between the JPM and JTL low, we can treat the elements as independent systems.

## V. SIMULATION RESULTS

The circuit shown in Fig. 2 was simulated in WRspice [24] and pscan2 [25]. Results of the pscan2 simulation of the full circuit are shown in Fig. 4. When the JPM is in the left well (qubit 0 state), the data pulse arrives at the DFF first, resulting in a logical 1 as an output. A subsequent reset pulse results in a logical 0, which is ignored. When the JPM is tilted into the right well (qubit 1 state), the clock pulse arrives at the DFF first, resulting in a logical 0 as an output. The reset pulse then results in logical 1, which is ignored. If an SFQ-DC converter is used to convert the measurement to a dc signal to be detected at room temperature, the entire sequence is repeated in order to toggle the SFQ-DC converter back into the off state.

Using pscan2 [25], a margin analysis can be performed to optimize parameter values. Optimized margins for junction area, inductance values, bias currents, and mutual inductances are shown in Table I. Margins greater than  $\pm 25\%$  are considered acceptable for the HYPRES fabrication process [26].

TABLE I  
OPTIMIZED PARAMETER MARGINS

junction area	[-40%, 40%]
inductances	[-26%, 38%]
bias currents	[-40%, 32%]
mutual inductances	[-37%, 40%]

## VI. CONCLUSION

We have developed a method for detecting the circulating current state of a JPM with SFQ logic. This method requires a relatively small number of standard SFQ cells, and only needs dc I/O lines on the cryostat. When a JPM is used for qubit measurement, as in [8], the combined circuit allows for a digital qubit readout that is single-shot, nearly quantum non-demolition [12], and immediately accessible at the same temperature stage as the qubit. This combined measurement method can form a key element for implementing a quantum-classical interface between an SFQ-based proximal classical coprocessor and a quantum array [3].

## ACKNOWLEDGMENT

This work was supported by the U.S. Government under Grant W911NF-15-1-0248; R.M. and B.L.T.P. acknowledge funding from the National Science Foundation under Grants QIS-1720304 and QIS-1720312, respectively.

## REFERENCES

- [1] R. Barends, J. Kelly, A. Megrant, A. Veitia, D. Sank, E. Jeffrey, T. C. White, J. Mutus, A. G. Fowler, B. Campbell, Y. Chen, Z. Chen, B. Chiaro, A. Dunsworth, C. Neill, P. O'Malley, P. Roushan, A. Vainsencher, J. Wenner, A. N. Korotkov, A. N. Cleland, and John M. Martinis. Superconducting quantum circuits at the surface code threshold for fault tolerance. *Nature*, 508(7497):500–503, 2014.
- [2] Maika Takita, Andrew W. Cross, A. D. Córcoles, Jerry M. Chow, and Jay M. Gambetta. Experimental Demonstration of Fault-Tolerant State Preparation with Superconducting Qubits. *Physical Review Letters*, 119(18):1–5, 2017.
- [3] R. McDermott, M. G. Vavilov, B. L.T. Plourde, F. K. Wilhelm, P. J. Liebermann, O. A. Mukhanov, and T. A. Ohki. Quantum-classical interface based on single flux quantum digital logic. *Quantum Science and Technology*, 3(2):1–16, 2018.
- [4] K. K. Likharev and V. K. Semenov. RSFQ Logic/Memory Family: A New Josephson-Junction Technology for Sub-Terahertz-Clock-Frequency Digital Systems. *IEEE Transactions on Applied Superconductivity*, 1(1):3–28, 1991.
- [5] R. McDermott and M. G. Vavilov. Accurate Qubit Control with Single Flux Quantum Pulses. *Physical Review Applied*, 2(1), 2014.
- [6] E. Leonard, M. A. Beck, J. Nelson, B.G. Christensen, T. Thorbeck, C. Howington, A. Opremcak, I.V. Pechenezhskiy, K. Dodge, N.P. Dupuis, M.D. Hutchings, J. Ku, F. Schlenker, J. Suttle, C. Wilen, S. Zhu, M.G. Vavilov, B.L.T. Plourde, and R. McDermott. Digital Coherent Control of a Superconducting Qubit. *Physical Review Applied*, 11(1):014009, 2019.
- [7] Y. F. Chen, D. Hover, S. Sendelbach, L. Maurer, S. T. Merkel, E. J. Pritchett, F. K. Wilhelm, and R. McDermott. Microwave photon counter based on josephson junctions. *Physical Review Letters*, 107(21):217401, 2011.
- [8] A. Opremcak, I. V. Pechenezhskiy, C. Howington, B. G. Christensen, M. A. Beck, E. Leonard, J. Suttle, C. Wilen, K. N. Nesterov, G. J. Ribeill, T. Thorbeck, F. Schlenker, M. G. Vavilov, B. L. T. Plourde, and R. McDermott. Measurement of a Superconducting Qubit with a Microwave Photon Counter. *Science*, 1242(September):1239–1242, 2018.
- [9] Alexandre Blais, RS Huang, and Andreas Wallraff. Cavity quantum electrodynamics for superconducting electrical circuits: An architecture for quantum computation. *Physical Review A*, 69(6), 6 2004.
- [10] T. Walter, P. Kurpiers, S. Gasparinetti, P. Magnard, A. Potočník, Y. Salathé, M. Pechal, M. Mondal, M. Oppliger, C. Eichler, and A. Wallraff. Rapid High-Fidelity Single-Shot Dispersive Readout of Superconducting Qubits. *Physical Review Applied*, 7(5):1–11, 2017.
- [11] K. B. Cooper, Matthias Steffen, R. McDermott, R. W. Simmonds, Seongshik Oh, D. A. Hite, D. P. Pappas, and John M. Martinis. Observation of Quantum Oscillations between a Josephson Phase Qubit and a Microscopic Resonator Using Fast Readout. *Physical Review Letters*, 93(18), 2004.
- [12] Luke C.G. Govia, Emily J. Pritchett, Canran Xu, B. L.T. Plourde, Maxim G. Vavilov, Frank K. Wilhelm, and R. McDermott. High-fidelity qubit measurement with a microwave-photon counter. *Physical Review A - Atomic, Molecular, and Optical Physics*, 90(6):62307, 2014.
- [13] Dmitri V. Averin, Kristian Rabenstein, and Vasili K. Semenov. Rapid ballistic readout for flux qubits. *Physical Review B - Condensed Matter and Materials Physics*, 73(9), 2006.
- [14] C. H. Van der Wal, A. C.J. Ter Haar, F. K. Wilhelm, R. N. Schouten, C. J.P.M. Harmans, T. P. Orlando, S. Lloyd, and J. E. Mooij. Quantum superposition of macroscopic persistent-current states. *Science*, 290(5492):773–777, 2000.
- [15] Arkady Fedorov, Alexander Shnirman, Gerd Schön, and Anna Kidiyarova-Shevchenko. Reading out the state of a flux qubit by Josephson transmission line solitons. *Physical Review B - Condensed Matter and Materials Physics*, 75(22):1–13, 2007.
- [16] Anna Herr, Arkady Fedorov, Alexander Shnirman, Evgeny Il'ichev, and Gerd Schön. Design of a ballistic fluxon qubit readout. *Superconductor Science and Technology*, 20(11), 2007.
- [17] I. I. Soloviev, N. V. Klenov, A. L. Pankratov, E. Il'ichev, and L. S. Kuzmin. Effect of Cherenkov radiation on the jitter of solitons in the driven underdamped Frenkel-Kontorova model. *Physical Review E - Statistical, Nonlinear, and Soft Matter Physics*, 87(6):1–5, 2013.
- [18] I. I. Soloviev, N. V. Klenov, S. V. Bakurskiy, A. L. Pankratov, and L. S. Kuzmin. Symmetrical Josephson vortex interferometer as an advanced ballistic single-shot detector. *Applied Physics Letters*, 105(20), 2014.
- [19] I. I. Soloviev, N. V. Klenov, A. L. Pankratov, L. S. Revin, E. Il'ichev, and L. S. Kuzmin. Soliton scattering as a measurement tool for weak signals. *Physical Review B - Condensed Matter and Materials Physics*, 92(1):1–8, 2015.
- [20] N. V. Klenov, A. V. Kuznetsov, I. I. Soloviev, S. V. Bakurskiy, M. V. Denisenko, and A. M. Satanin. Flux qubit interaction with rapid single-flux quantum logic circuits: Control and readout. *Low Temperature Physics*, 43(7):789–798, 2017.
- [21] Kirill G. Fedorov, Anastasia V. Shcherbakova, Michael J. Wolf, Detlef Beckmann, and Alexey V. Ustinov. Fluxon readout of a superconducting qubit. *Physical Review Letters*, 112(16):1–5, 2014.
- [22] Samuel Intiso, Jukka Pekola, Alexander Savin, Ygor Devyatov, and Anna Kidiyarova-Shevchenko. Rapid single-flux-quantum circuits for low noise mK operation. *Superconductor Science and Technology*, 19(5):S335–S339, 5 2006.
- [23] S.V. Rylov, L.a. Bunz, D.V. Gaidarenko, M.a. Fisher, R.P. Robertazzi, and O.a. Mukhanov. High resolution ADC system. *IEEE Transactions on Applied Superconductivity*, 7(2):2649–2652, 1997.
- [24] Stephen Whiteley. wrcad.com.
- [25] Pavel Shevchenko. pscan2sim.org.
- [26] HYPRES Design Rules: <https://www.hypres.com/wp-content/uploads/2010/11/DesignRules-6.pdf>.